Applied Catalysis B: Environmental 256 (2019) 117782

Contents lists available at ScienceDirect

Applied Catalysis B: Environmental

journal homepage: www.elsevier.com/locate/apcatb

Surface Fe(III)/Fe(II) cycle promoted the degradation of atrazine by peroxymonosulfate activation in the presence of hydroxylamine

Jun Li[a,c], Yanjian Wan[b], Yangju Li[a,c], Gang Yao[c,d], Bo Lai[a,c,*]

[a] State Key Laboratory of Hydraulics and Mountain River Engineering, College of Architecture and Environment, Sichuan University, Chengdu 610065, China
[b] Institute of Environmental Health, Wuhan Centers for Disease Prevention & Control, Wuhan, 430022, China
[c] Sino-German Centre for Water and Health Research, Sichuan University, Chengdu, 610065, China
[d] Institute of Environmental Engineering, RWTH Aachen University, Aachen, 52072, Germany

ARTICLE INFO

Keywords:
Atrazine
Fe_3O_4
Peroxymonosulfate
Hydroxylamine
Surface
Fe(III)/Fe(II)cycle

ABSTRACT

In this study, we demonstrated that Fe_3O_4/PMS system in the presence of hydroxylamine (HA) was significantly efficient for atrazine degradation under the near-neutral pH (5.0–6.8) (without buffer). The degradation rate constant of atrazine in Fe_3O_4/PMS/HA system (0.152 min^{-1}) was 38 times of that (0.004 min^{-1}) in Fe_3O_4/PMS system and even 4.75 times of that (0.032 min^{-1}) in HA/PMS system. In this Fe_3O_4/PMS/HA system, the roles of HA were mainly two parts. On one hand, 40% atrazine was decomposed through the activation of peroxymonosulfate (PMS) by HA as a metal-free activator. On the other hand, the addition of HA could highly promote the surface Fe(III)/Fe(II) cycle on the Fe_3O_4. Meanwhile, the trace dissolved Fe^{2+} was not the major reason for the atrazine degradation. The reason for different atrazine degradation efficiencies under various aeration conditions was analyzed, which showed that the reduced molecular oxygen was more conducive to accelerate the regeneration of surface Fe(II). Subsequently, the transformation products of HA under different aeration conditions were monitored. What's more, the reactive species were detected by electron paramagnetic resonance (EPR) and quenching experiments, which revealed that both sulfate radical ($SO_4^{\bullet-}$) and hydroxyl radical ($HO^{\bullet}$) were responsible for the atrazine degradation, especially sulfate radical. Finally, the reaction mechanism of Fe_3O_4/PMS/HA system based on the Fe(III)/Fe(II) cycle and the metal-free activation was proposed according to the comprehensive analysis. This study provides an efficient degradation of atrazine organic pollutant in water by the heterogeneous Fenton-like system.

1. Introduction

Atrazine (2-chloro-4-ethylamino-6-isopropylamino-1, 3, 5-triazine) is one of the most common herbicides and is widely used to control broadleaf weeds in crop fields. Its widespread use has caused serious water contamination in surface water and groundwater [1]. Because the persistent atrazine herbicide has the property of relative long half-life (about 30–100 days), moderate aqueous solubility, low biodegradability, and high leaching potential [2,3], the commercial use of atrazine in some European countries has been banned. Meanwhile, it has been listed as the priority list of 76 substances in European Union Water Framework Directive [4]. However, its presence in contaminated surface and ground water will exist for a long time in the absence of any water treatment technologies intervention. In addition, in China, the atrazine detection concentration in the surface and ground water was always 0.12–5.16 μg/L in Beijing, even exceeding the maximum allowed level in the drinking water (3 μg/L) [5]. Thus, it is important to eliminate atrazine in water.

In recent years, sulfate radical based advanced oxidation processes ($SO_4^{\bullet-}$-AOPs) have gained increasing attentions to degrade the organic pollutants in surface and ground water. Sulfate radical ($SO_4^{\bullet-}$) has been regarded as a powerful oxidant with the oxidation potential of 2.5–3.1 V, which is even higher than the oxidation potential of hydroxyl radical ($HO^{\bullet}$) [6]. In addition, compared with hydroxyl radical, sulfate radical is more efficient than hydroxyl radical to degrade organic contaminant with a wide range pH of 2–8. Moreover, the half-time of sulfate radical (30–40 μs) is much higher than that of hydroxyl radical (< 1 μs), which makes the sulfate radical a better reaction with the targeted compounds [7,8]. Importantly, peroxymonosulfate (PMS) as one of the main sources of sulfate radical has been studied widely [9–11]. Homogeneous catalytic oxidation by PMS activation applied for water treatment is efficient. Especially, because of the environmental

* Corresponding author at: State Key Laboratory of Hydraulics and Mountain River Engineering, College of Architecture and Environment, Chengdu, 610065, China.
E-mail address: laibo@scu.edu.cn (B. Lai).

https://doi.org/10.1016/j.apcatb.2019.117782
Received 11 January 2019; Received in revised form 28 April 2019; Accepted 25 May 2019
Available online 29 May 2019
0926-3373/

friendliness and high catalytic activity, Fe^{2+} has been used as the most common activator of PMS for water treatment [12]. Nevertheless, the regeneration of Fe^{2+} is the rate-limiting step for pollutant degradation [13]. In order to improve the regeneration of Fe^{2+} and reduce the yield of iron sludge, some researchers found that the reducing agent, such as hydroxylamine (HA), could greatly promote the cycle of Fe^{3+} to Fe^{2+} in homogeneous catalytic oxidation process [13–15]. Similarly, Lee et al. [16] reported the degradation of recalcitrant organic contaminants by the nonselective Cu(III) species generated in the Cu(II)/HA and Cu(II)/H_2O_2/HA homogeneous systems. However, the homogeneous catalytic oxidation processes have some drawbacks, such as a large amount of catalyst ions, secondary pollution, and difficulty in catalyst recovery, etc.

To further overcome the defects of homogeneous catalytic oxidation, the studies about hydroxylamine applied in the heterogeneous catalytic oxidation process have been the research focus [17,18]. Importantly, taking iron-based materials as the example, it has been reported that the catalytic activity of iron-based heterogeneous Fenton catalysts have a positive correlation with the surface Fe(II) content and/or the Fe(III)/Fe(II) cycle performance of iron-based materials [19]. Unfortunately, the problem of efficient surface Fe(II) regeneration also exists in the iron oxide-based heterogeneous catalytic oxidation, which results in many iron oxides showing poor activity for the PMS activation [20]. Fe_3O_4 magnetite nanoparticle is the inverse spinel structure with both Fe(II) and Fe(III), guaranteeing the reversible oxidation and reduction of the Fe(II) and Fe(III) while keeping the structure unchanged during the PMS activation process [20]. Previously, Zhang et al. [21] investigated the orange G degradation through peroxymonosulfate activation by magnetite nanoparticles in the presence of hydroxylamine. However, the mechanism of the reaction system needs further research in depth. Herein, we introduce the Fe_3O_4/PMS Fenton-like system in the presence of hydroxylamine, which might accelerate the surface Fe(III) and Fe(II) cycle on Fe_3O_4, thereby degrading atrazine rapidly and efficiently through the heterogeneous catalytic process. The objectives of this study are to: (i) assess the main roles (reducing agent or activator) of HA with different concentration during the atrazine degradation in the Fe_3O_4/PMS/HA system; (ii) identify the differences of transformation products (i.e., N_2O, N_2, NO_2^-, and NO_3^-) of hydroxylamine in Fe_3O_4/PMS/HA system under different aeration conditions; (iii) confirm the surface Fe(III)/Fe(II) cycle on Fe_3O_4 by X-ray photoelectron spectroscopy; (iv) explore the reaction mechanism of Fe_3O_4/PMS/HA heterogeneous system.

2. Materials and methods

2.1. Reagent

The commercial Fe_3O_4 was used in our experiments. The detailed information of other reagents is shown in the Supporting Information Text S1.

2.2. Experimental procedures

Atrazine stock solution (23 μM) was prepared by dissolving atrazine in ultrapure water (18.2 MΩ. cm) and storing it in dark to avoid any photochemical degradation. The degradation experiments were conducted in 200 mL flat bottom beaker (or three-necked flask, if needed) with a constant stirring speed (250 rpm), keeping the reaction temperature at 25 ± 0.2 ℃ by water batch heating. The reaction was triggered by introducing the desired Fe_3O_4, HA, PMS, and buffer (if needed) into the atrazine solution. Meanwhile, the solution pH was not adjusted unless otherwise stated. In addition, for the experiments of studying the influence of molecular oxygen on atrazine degradation, the reaction solutions were aerated by N_2 and O_2 (200 mL/min) for 30 min before the reaction start, respectively. During the reaction process, samples were taken out at different time intervals with syringes and filtered through 0.45 μm polytetrafluoroethylene (PTFE) syringe filter discs. Ethanol was used to quench the degradation reaction before analyzing by high performance liquid chromatography (HPLC). All of the degradation experiments were replicated three times.

2.3. Analytical methods

The atrazine concentration was determined by HPLC (Agilent USA) with the Eclipse XDB C-18 (5 μm, 4.6 × 250 mm) at a UV wavelength of 225 nm. The mobile phase included ultrapure water and methanol at a volume ratio of 20:80 (v/v) with a flow rate of 1.0 mL/min. The injection volume was 20 μL and the column temperature was set at 25 ˚C. Hydroxylamine was firstly reacted with acetone to form acetoxime, and then measured on the same HPLC at 220 nm and a mixture (0.8 mL/min) of methanol and ultrapure water (70:30, v/v). The specific surface area of Fe_3O_4 used in our experiments is 9.3 m^2/g, which was calculated based on Brunauer-Emmett-Teller (BET) model with a specific surface area analyzer (Micromeritics ASAP 2460). The total iron ions concentration was detected by inductively coupled plasma optical emission spectrometer (Agilent, ICP-OES 5100 SVDV). The dissolved Fe^{3+} ions concentration in the solution was evaluated quantitatively by a 1,10-phenanthroline method with a UV–vis spectrophotometer (752 N, INESA, Shanghai, China) [18]. The dissolved oxygen (DO) concentration in the reaction solution was determined by HQ30d (HACH, Loveland, CO, USA) oxygen meter, and the DO concentration in atrazine solution in the physical condition was 6.9–7.5 mg/L. The pH_{pzc} (point of zero charge) of Fe_3O_4 was measured by nano-particle size Zeta potentiometer. Electron paramagnetic resonance (EPR) spectra were obtained with a Bruker EMX plus X-band CW EPR spectrometer at room temperature with DMPO as the radical spin-trapping reagent. The concentration of dissolved N_2O was measured using a microsensor (UNISENSE). The NO_3^- and NO_2^- concentration were determined by SKALAR SAN + + continuous flowing analyzer. The H_2O_2 concentration was detected by the titanium oxysulfate method at 405 nm by UV–vis spectrophotometer (UV-1800, Shimadzu, Japan) [22]. The concentration of residual PMS was determined by the modified iodometric method at pH 2.0 [23]. The atrazine degradation intermediates were detected by Waters QTOF (Waters ACQUITY UPLC I-Class coupled with Xevo G2-XS QTOF, Waters Corporation, Milford, MA, USA), which is shown in the Supporting Information Text S2. The measurement of superoxide radical and the characterization method of Fe_3O_4 are shown in the Supporting Information Text S2.

3. Results and discussion

3.1. Characterization of Fe_3O_4

Fig. S1(a) and (b) show that the obtained commercial Fe_3O_4 are nanoscale particles, which corresponded to the standard crystalline Fe_3O_4 (JCPDS 19-0629). Detailed results and discussions are shown in the Supporting Information Text S3.

3.2. Atrazine degradation in different systems

3.2.1. The comparative study of atrazine degradation

The atrazine degradation curves in different systems are compared and demonstrated in Fig. 1(a). It was found that almost no atrazine degradation was shown in Fe_3O_4/HA system. Only 10% atrazine was degraded in Fe_3O_4/PMS system, suggesting the slight catalytic effect of Fe_3O_4 for peroxymonosulfate due to the poor surface Fe(III)/Fe(II) cycle of Fe_3O_4 [24]. What's more, about 40% atrazine was degraded in HA/PMS system, which was due to the generation of radicals through reaction between HA and PMS [23]. Importantly, nearly 94% atrazine was degraded in the Fe_3O_4/PMS/HA system. The degradation of atrazine corresponded to the pseudo-firstorder reaction kinetics in the above systems. For comparison, we also investigated the apparent

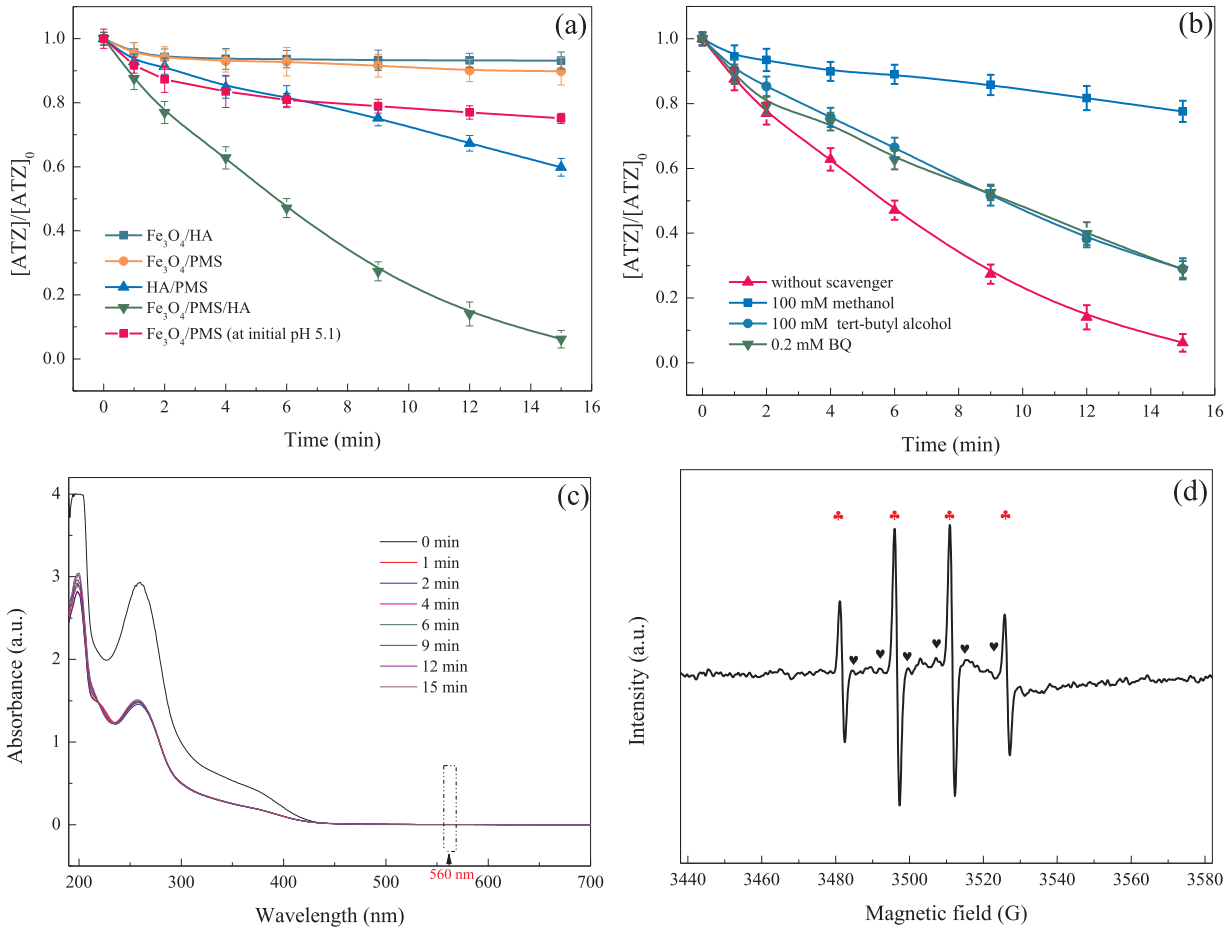

Fig. 1. (a) Atrazine degradation in the different systems, (b) quenching experiments, (c) the UV spectra of NBT solution reacted with samples, and (d) EPR spectra in the Fe_3O_4/PMS/HA system. Experiment conditions: $[atrazine]_0$ = 23 μM, $[Fe_3O_4]_0$ = 0.69 g/L, $[HA]_0$ = 0.3 mM, $[PMS]_0$ = 0.4 mM, initial pH = 6.8 (without buffer), and reaction time = 15 min.

degradation rate constant (k_{obs}) (Fig. S2). Obviously, k_{obs} (0.152 min^{-1}) in Fe_3O_4/PMS/HA system was higher than the simple sum of those by the Fe_3O_4/PMS (0.004 min^{-1}) and Fe_3O_4/HA (0.005 min^{-1}) systems, and even almost 4.75 times of that (0.032 min^{-1}) in HA/PMS system. Because the reaction solution pH would change with the addition of hydroxylamine hydrochloride (HA) due to the release of H^+ ions from the HA dissolution, the variation of pH caused by HA addition was examined. We set up another experiment to explore whether the high atrazine degradation in Fe_3O_4/PMS/HA system was caused by the enhancement of Fe_3O_4/PMS system under acidic condition. It is found that the solution pH decreased quickly from 6.8 to 5.1 as soon as 0.3 mM HA was added to the reaction solution. To evaluate the effect of pH condition, we explore the atrazine degradation efficiency in Fe_3O_4/PMS system at initial pH 5.1. Under this condition, the atrazine degradation efficiency was only 25% after 15 min treatment, which was still significantly lower than that (94%) in Fe_3O_4/PMS/HA system, suggesting that although the release of H^+ ions from HA can be in favor of atrazine degradation slightly, it is not the main reason for strengthening the catalytic oxidation capacity for atrazine degradation.

3.2.2. Main radicals responsible for atrazine degradation

Hydroxyl radical ($HO^{\bullet}$), sulfate radical ($SO_4^{\bullet-}$), superoxide radical ($O_2^{\bullet-}$), and peroxymonosulfate radical ($SO_5^{\bullet-}$) are considered as the possible radicals in the PMS activations [25–27]. Thus, we further investigated the main radicals produced in Fe_3O_4/PMS/HA system. 1, 4-Benzoquinone (BQ), tertiary butanol (TBA), and methanol (MeOH) were used as the three radical scavengers ($O_2^{\bullet-}$, $HO^{\bullet}$, and both $HO^{\bullet}$ and $SO_4^{\bullet-}$, respectively) to check the generation of radicals due to the different reaction rates between them and the free radicals [17]. $SO_5^{\bullet-}$ might be formed in the system, however, $SO_5^{\bullet-}$ is usually not considered to be responsible for the degradation of atrazine because of its low oxidation ability ($E(SO_5^{\bullet-}/SO_4^{2-})$ = 1.1 V) [28,29]. In Fig. 1(b), regard to the Fe_3O_4/PMS/HA system, when 100 mM TBA and MeOH were added into the solution, the atrazine degradation efficiency was inhibited from 94% to 71% and 22%, respectively, indicating that both hydroxyl radical and sulfate radical participated in the destruction of atrazine, but sulfate radical was the main free radical in the system. Meanwhile, atrazine degradation decreased to about 71% in the presence of 0.2 mM BQ. However, since BQ also could react with the hydroxyl radicals and sulfate radicals ($k_{SO4\bullet-}$ = $1 \times 10^8 M^{-1}s^{-1}$, $k_{HO\bullet}$ = 6.6×10^9 M^{-1} s^{-1}) [30,31], the inhibition of atrazine degradation by BQ addition could not effectively prove the existence of $O_2^{\bullet-}$ based on the above results. In order to further explore whether $O_2^{\bullet-}$ contributed to atrazine degradation, we further conducted the $O_2^{\bullet-}$ measurement experiments. Nitro blue tetrazolium (NBT) is a widely used reagents for the $O_2^{\bullet-}$ concentration detection based on the absorbance at wavelength of 560 nm by the reaction of NBT and $O_2^{\bullet-}$ [32,33]. As shown in Fig. 1(c), the absorbance at 560 nm was zero, indicating that there was no $O_2^{\bullet-}$ generated in Fe_3O_4/PMS/HA system.

Subsequently, electron paramagnetic resonance (EPR) experiment with DMPO as a spin trap agent was further used to detect the radicals generated in the Fe_3O_4/PMS/HA system based on the detection principle that DMPO would capture hydroxyl radical and sulfate radical in solution to generate the DMPO−$HO^{\bullet}$ and DMPO − $SO_4^{\bullet-}$ adducts. As noted in Fig. 1(d), four characteristic peaks of DMPO−$HO^{\bullet}$ adduct with

a peak height ratio of 1:2:2:1 and the hyperfine splitting parameters were $\alpha_N = \alpha_H = 14.9$ G, suggesting that hydroxyl radical was generated in the system [34]. Also, the special hyperfine coupling constants of $a_N = 13.8$ G, $a_H = 10.1$ G, $a_H = 1.4$ G, and $a_H = 0.8$ G was in accordance with DMPO − $SO_4^{\bullet-}$ adduct, indicating the generation of sulfate radical [35]. The above results confirmed that both hydroxyl radical and sulfate radical were generated in the Fe_3O_4/PMS/HA system.

Based on the above discussion, the atrazine degradation could be expressed as follows (Eqs. (1) and (2)):

$$-\frac{d[ATZ]}{dt} = k_{PMS}[PMS][ATZ] + k_{cata}[cata][ATZ] + k_{HO\bullet}[HO^{\bullet}][ATZ] + k_{SO4\bullet-}[SO_4^{\bullet-}][ATZ] = k_{obs}[ATZ] \quad (1)$$

$$k_{obs} = k_{PMS}[PMS] + k_{cata}[cata] + k_{HO^{\bullet}}[HO^{\bullet}] + k_{SO_4^{\bullet-}}[SO_4^{\bullet-}] \quad (2)$$

where k_{PMS}, $k_{HO\bullet}$, and $k_{SO4\bullet-}$ (M^{-1} s^{-1}) are degradation constants of atrazine by PMS, $HO^{\bullet}$, and $SO_4^{\bullet-}$, respectively. k_{cata} is the adsorption rate constant $(g/L)^{-1}$ s^{-1} of atrazine by Fe_3O_4 catalyst. [ATZ], [$HO^{\bullet}$], and [$SO_4^{\bullet-}$] are the concentration of atrazine, $HO^{\bullet}$, and $SO_4^{\bullet-}$, respectively. In this study, the atrazine degradation by Fe_3O_4 adsorption and PMS oxidation were negligible, therefore, the k_{cata} and k_{PMS} are assumed to be zero. $k_{HO\bullet}$, and $k_{SO4\bullet-}$ are 3.0×10^9 M^{-1} s^{-1} [36] and the Eq. (2) could be simplified to the following Eq. (3):

$$k_{obs} = k_{HO^{\bullet}}[HO^{\bullet}] + k_{SO_4^{\bullet-}}[SO_4^{\bullet-}] = k_{HO^{\bullet}-SO_4^{\bullet-}}([HO^{\bullet}] + [SO_4^{\bullet-}]) \quad (3)$$

According to Eqs. (1)–(3), it was found that the sum concentration (8.433×10^{-7} μM) of sulfate radical and hydroxyl radical for atrazine degradation in the Fe_3O_4/PMS/HA system was nearly 40 times of that (2.12×10^{-8} μM) in the Fe_3O_4/PMS conventional Fenton-like system and even almost 4.8 times of that (1.767×10^{-7} μM) in HA/PMS system (data not shown), further confirming that HA plays an indispensable role in promoting free radicals formation for atrazine degradation. It has been reported that HA could reduce the surface Fe(III) into Fe(II) on FeOOH to accelerate the regeneration of Fe(II) [18]. Thus, we hypothesized that the improvement of atrazine degradation in Fe_3O_4/PMS in the presence of HA was mainly ascribed to the accelerated Fe(III)/Fe(II) cycle on the surface of Fe_3O_4. Subsequently, the performance of Fe_3O_4/PMS/HA system for atrazine degradation was systematically elucidated based on the Fe_3O_4 dosage, PMS concentration, HA concentration, initial pH, and aeration conditions.

3.3. Fe_3O_4 dosage and PMS concentration effects on the atrazine degradation in the Fe_3O_4/PMS/HA system

In Fig. S3 and Figs. S4 (a–b), the increase of Fe_3O_4 dosage from 0 to 0.69 g/L and PMS concentration from 0 to 0.4 mM enhanced the atrazine degradation efficiency. However, the further improvement of Fe_3O_4 catalyst and PMS would inhibit the destruction of atrazine. Detailed results and discussions are shown in the Supporting Information Text S4.

3.4. HA concentration effects on the atrazine degradation in the Fe_3O_4/PMS/HA system

The effects of HA concentration (0, 0.1, 0.2, 0.3, 0.4, 0.5, 0.8, and 1.0 mM) on atrazine degradation in Fe_3O_4/PMS/HA system are illustrated in Fig. 2. The increased atrazine degradation efficiency was shown with the enhanced HA concentration ranging from 0 to 0.5 mM, and then it nearly leveled off with HA further changing from 0.5 to 1.0 mM (Fig. 2(a)). In addition, it should be noted that increased degradation reaction rate (k_{obs} from 0.004 to 0.302 min^{-1}, Fig. S4(c)) in the Fe_3O_4/PMS/HA system was observed with the improved HA concentration from 0 to 1.0 mM. Meanwhile, we also compared the variation of solution pH in the Fe_3O_4/PMS/HA system during 15 min in the presence of 0.3 mM and 1.0 mM HA with other parameters identical, respectively. As shown in the Fig. S5(b), the solution pH values in the Fe_3O_4/PMS/HA system with 0.3 mM HA was similar with that of 1.0 mM, indicating that the increase in the atrazine degradation accompanied by the increase of HA concentration is not due to pH changes. In spite of the obvious improvement of atrazine degradation, Feng et al. [23] have demonstrated that HA could activate PMS to generate radicals. Herein, the HA/PMS system was introduced at the same PMS concentration (0.4 mM) and different HA concentration (0, 0.1, 0.2, 0.3, 0.4, 0.5, 0.8, and 1.0 mM) to further evaluate the role of HA in Fe_3O_4/PMS/HA system. Interesting, in Fig. 2(b), it is found that the atrazine degradation efficiency increased from 30% to 63% and k_{obs} enhanced from 0.023 to 0.063 min^{-1} with HA concentration increasing from 0.1 to 1.0 mM in HA/PMS system (Fig. S4(d)), suggesting that the PMS activation was enhanced with the increasing HA concentration.

Based on the aforementioned analysis, the proportion of atrazine degradation efficiency depended on the Fe(III)/Fe(II) recycle reduced by HA in the Fe_3O_4/PMS/HA system was explored. Herein, the roles of hydroxylamine were divided into two parts in Fe_3O_4/PMS/HA system, (i) the activation for PMS: the corresponding atrazine degradation efficiency was expressed as DEa; (ii) the reduction of Fe(III) into Fe(II): the corresponding atrazine degradation efficiency was represented as DEr. Fig. 2(c) illustrates the difference value of atrazine degradation efficiency in Fe_3O_4/PMS/HA and HA/PMS systems with the identified conditions unless the Fe_3O_4 dosage. It showed that the DEa accounting in the whole atrazine degradation efficiency kept growing. The DEr showed a trend of going up first, reaching the maximum (54%) at 0.3 mM HA, and then down when HA concentration exceeded 0.3 mM. When HA concentration was 0.5 mM, the DEa and DEr in the whole atrazine degradation efficiency were half and half. The results suggested that the main role of HA was to accelerate the surface Fe(III)/Fe(II) recycle before the HA concentration increased to 0.5 mM, and HA would primarily act as a metal-free activator for PMS when HA concentration exceeded 0.5 mM.

3.5. Initial pH effects on the atrazine degradation in the Fe_3O_4/PMS/HA system

The solution pH significantly affects the ion species distribution and the generation of radical. Herein, considering the addition of PMS and HA would immediately decrease solution pH, we investigated the atrazine degradation in Fe_3O_4/PMS/HA system at different initial pH with buffer and without buffer. (i) Atrazine degradation without buffer: for all studied initial pH, the solution pH rapidly decreases in the first seconds and sustain unchanged. In Fig. 3(a), it found that the atrazine degradation in Fe_3O_4/PMS/HA system was obviously pH dependent. The highest atrazine degradation (about 94%) was obtained under near-neutral pH (6.8 and 5.0), while it was dramatically inhibited at both acidic pH (pH ≤ 3) and high-alkaline pH (≥ 9.0) ranges. Specifically, there was almost no atrazine removal at initial 11.0 and 2.0, only reaching 8% and 19%, respectively. In addition, the apparent degradation rate constant (k_{obs} = 0.152 min^{-1}) at neutral pH 6.8 is 55 and 6 times of those at initial pH 11.0 (0.002 min^{-1}) and 2.0 (0.027 min^{-1}), respectively (Fig. S4(e)). Thus, in this Fe_3O_4/PMS/HA system, neither strong acid nor high alkaline pH was conducive to the degradation of atrazine. We therefore monitored the pH variation during the atrazine degradation with different initial pH (Fig. 3(b)). It can be seen that the pH value remained unchanged in the first 30 s and kept at 4.9 and 10.5 when the initial pH of reaction solutions were 9.0 and 11.0, respectively. The pK_a values of HA are 5.96 and 13.74 [37]. From Fig. S6(a), the fraction of NH_2OH have increased with initial pH ≥ 9.0 and NH_2OH was almost the only NH_2OH species at pH 11.0. Because NH_2OH has a high reaction rate with hydroxyl radical and sulfate radical ($k = 9.5 \times 10^9$ $M^{-1}s^{-1}$ for $HO^{\bullet}$ [28], $k = 8.5 \times 10^8$ $M^{-1}s^{-1}$ for $SO_4^{\bullet-}$ [38]), which was comparable to that between above radicals and atrazine ($k = 3 \times 10^9$ $M^{-1}s^{-1}$ for $HO^{\bullet}$ and $SO_4^{\bullet-}$) [36], resulting most generated free radicals were consumed without

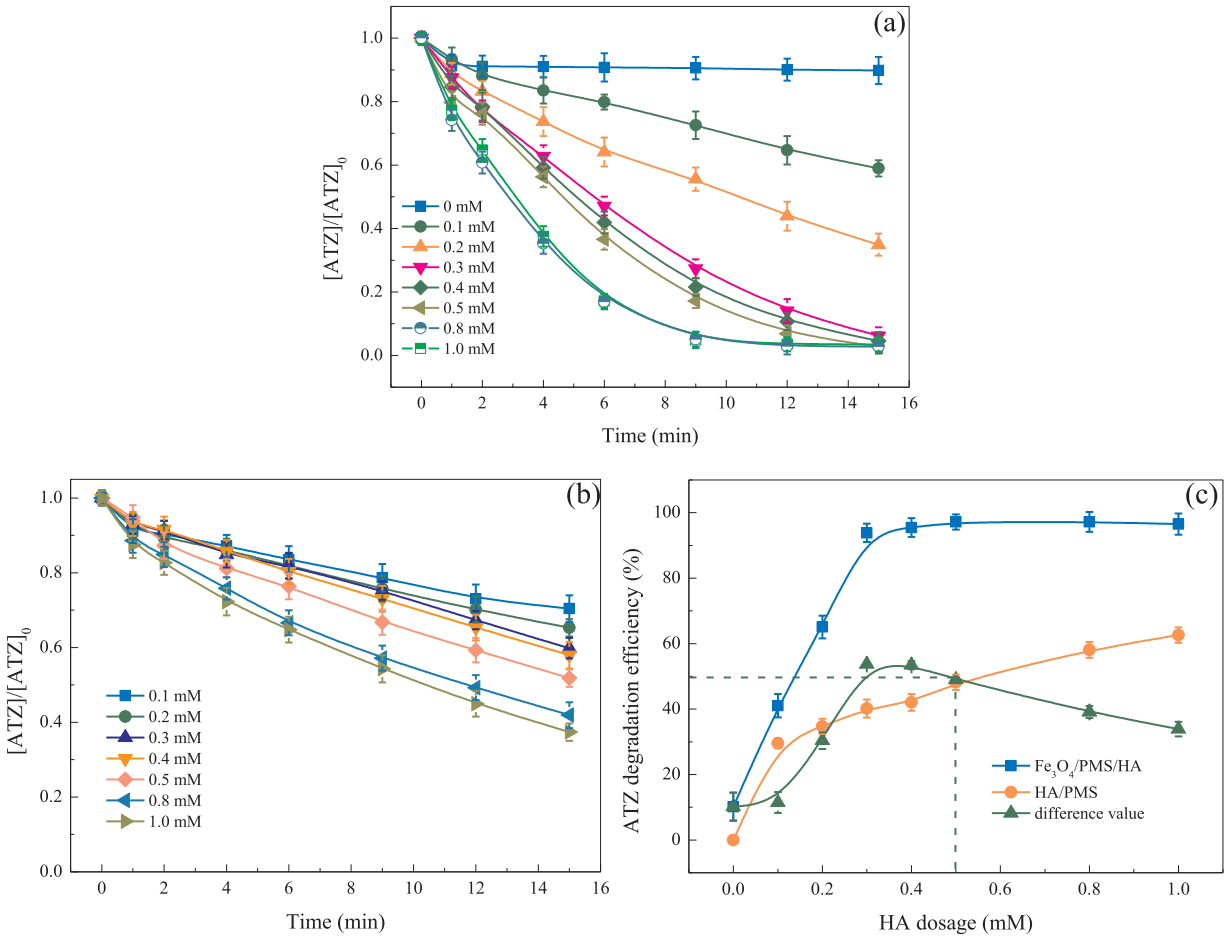

Fig. 2. Effects of HA concentration on atrazine degradation in (a) Fe_3O_4/PMS/HA system and (b) HA/PMS system, and (c) the difference value of atrazine degradation efficiency in different systems. Experiment conditions: $[atrazine]_0$ = 23 μM, $[Fe_3O_4]_0$ = 0.69 g/L, $[PMS]_0$ = 0.4 mM, initial pH = 6.8 (without buffer), and reaction time = 15 min.

attacking the pollutants. Moreover, pKa_1 of H_2SO_5 is less than 0 and the pK_{a2} value is 9.4 [39]. Thus, dianion form (SO_5^{2-}) was the main existence form of PMS when the reaction solution was at pH 10.5 (Fig. S6(b)). Meanwhile, the pH_{pzc} of Fe_3O_4 was detected to be around 5.0 (Fig. S7). The electrostatic repulsion between Fe_3O_4 and SO_5^{2-} reduced the chance of interacting with each other, further reducing the atrazine degradation efficiency compared with that at initial 9.0.

At initial pH < 5, the solution pH during the reaction process nearly have no change compared with the initial pH. Under the condition, monoanion form (HSO_5^-) was the dominant existing form of PMS in

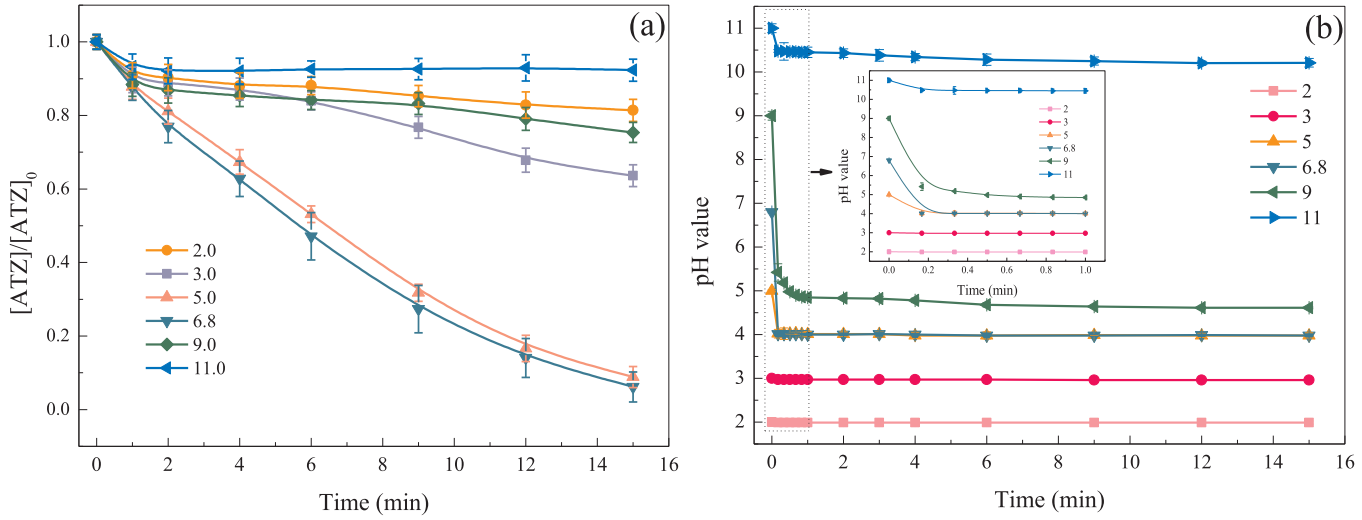

Fig. 3. (a) Effects of initial solution pH (without buffer) on atrazine degradation in Fe_3O_4/PMS/HA system, and (b) variation of solution pH during the reaction time with different initial pH (without buffer). Experiment conditions: $[atrazine]_0$ = 23 μM, $[Fe_3O_4]_0$ = 0.69 g/L, $[HA]_0$ = 0.3 mM, $[PMS]_0$ = 0.4 mM, and reaction time = 15 min.

the reaction solution (Fig. S6(b)) and the catalyst was also positively charged. In this way, the lower pH (2 and 3) should be in favor of the atrazine degradation for the enhancement of electrostatic interaction between PMS and Fe_3O_4. However, the fact is that atrazine degradation efficiency dramatically decreased. It was due to the adverse effect of H^+ on the PMS activation process [40,41]. The hydrogen bond formed between H^+ and the O—O group of HSO_5^- would play a vital role at pH ≤ 3, attaching a positive charge to HSO_5^- and eventually hindering its interaction with the positively charged oxide surface [39]. The similar inverse H^+-dependency phenomenon in PMS activation systems also have been reported [42,43]. (ii) Atrazine degradation with buffer: meanwhile, the effects of initial pH with buffer solution on the atrazine degradation are shown. In the Fig. S8, the optimal degradation efficiency (95%) was obtained under the pH 4.0, which was corresponding to the initial pH 5.0 and 6.8 without buffer (Fig. 3). In other words, the relationship between the atrazine degradation efficiency and the actual pH of the solution was consistent regardless of whether or not a buffer solution was added. Herein, in order to avoid the introduction of other ions, the following experiments do not use buffer solution unless otherwise specified.

3.6. Molecular oxygen effects on the atrazine degradation in the Fe_3O_4/PMS/HA system

3.6.1. Atrazine degradation under different aeration conditions

Because molecular oxygen could affect the generation of hydrogen peroxide and the cycle of surface Fe(III)/Fe(II) [16,18], the atrazine degradation in Fe_3O_4/PMS/HA system were performed with the N_2 condition, physical condition, and O_2 condition, respectively (Fig. 4(a)). The reaction solution of Fe_3O_4/PMS/HA-N_2 (or O_2) system was aerated with high-purity N_2 (or O_2) for 30 min before the reaction started and purged with N_2 (or O_2) constantly during the 15 min reaction process. The degradation efficiency of atrazine reached > 99% in the shortened 12 min under the anoxic condition in the Fe_3O_4/PMS/HA-N_2 system. In contrast, when O_2 was bubbling into the reaction solution, the degradation of atrazine was inhibited and only 82% atrazine was degraded in the 15 min. All of the atrazine degradations obeyed pseudo-first order kinetics (Fig. S4(f)). The degradation rate constant of atrazine within 12 min in the Fe_3O_4/PMS/HA-N_2 system was calculated to be 0.220 min^{-1}, which was about 1.5 times of that (0.152 min^{-1}) in Fe_3O_4/PMS/HA system and even 2.0 times of that (0.111 min^{-1}) in the Fe_3O_4/PMS/HA-O_2 system, suggesting that the presence of molecular oxygen could inhibit the atrazine degradation in this Fe_3O_4/PMS/HA system, probably as the molecular oxygen restrained the cycle of surface Fe(III)/Fe(II) on catalyst. Meanwhile, we also calculated the specific surface area normalized degradation rate constant ($k_{ssa\text{-}obs}$), the $k_{ssa\text{-}obs}$ in the Fe_3O_4/PMS/HA system under N_2 condition, physical condition, and O_2 condition were 0.024, 0.016, and 0.012 g min^{-1} m^{-2}, respectively. (Table S1). Also, the HA and PMS decomposition in the above three systems were evaluated (Fig. S9(a) and (b)). The decomposition efficiency of both HA and PMS show the same trend in the above three systems: Fe_3O_4/PMS/HA-N_2 system > Fe_3O_4/PMS/HA system > Fe_3O_4/PMS/HA-O_2 system, which was obviously in accordance with the atrazine degradation in their systems.

For the different atrazine degradation, we firstly suspected whether the reaction systems under different aeration conditions would produce different kinds of free radicals and cause different atrazine degradation. Thus, we investigated the main free species responsible for atrazine degradation in the three different systems. As seen in Fig. 4(b), about 94% atrazine was degraded without any scavenger addition in Fe_3O_4/PMS/HA system. The addition of 0.2 mM BQ shows an inhibition on the atrazine degradation after 15 min treatment. However, since BQ could react with the hydroxyl radicals and sulfate radicals ($k_{SO4\cdot-} = 1 \times 10^8 M^{-1}s^{-1}$, $k_{HO\cdot} = 6.6 \times 10^9$ M^{-1} s^{-1}) [30,31], the inhibition of atrazine degradation by BQ addition could not effectively prove the existence of $O_2^{\cdot-}$ based on the above results. In order to further explore whether $O_2^{\cdot-}$ contribute to atrazine degradation, we conducted the $O_2^{\cdot-}$ measurement experiments by nitro blue tetrazolium (NBT). As shown in Fig. S10(a–c), in the Fe_3O_4/PMS/HA system under three aeration conditions (physical, O_2, and N_2), the absorbance of samples at 560 nm was zero, indicating that there was no $O_2^{\cdot-}$ generated in the studied systems. Meanwhile, in all the three systems, when 100 mM TBA and MeOH were added into the reaction solution, respectively, all three systems show the similar the phenomena that inhibitory effect of atrazine degradation by MeOH was much higher than that of TBA, indicating that there are no differences in the free radicals produced in the Fe_3O_4/PMS/HA-N_2, Fe_3O_4/PMS/HA, and Fe_3O_4/PMS/HA-O_2 systems and the atrazine degradation in the Fe_3O_4/PMS/HA system under different aeration conditions was depended on the attack of hydroxyl radical and sulfate radical, especially sulfate radical. In other words, the radical species in the three systems were not the main cause of different atrazine degradation efficiency under three aeration conditions.

3.6.2. Confirmation of surface Fe(III)/Fe(II) cycle

As reported in the literatures, hydrogen peroxide (H_2O_2) would be formed by O_2 reduction even if the formation rate is very slow (Eqs. (4) and (5)) [16,44,45]. Chen et al. [46] reported that the hydrogen

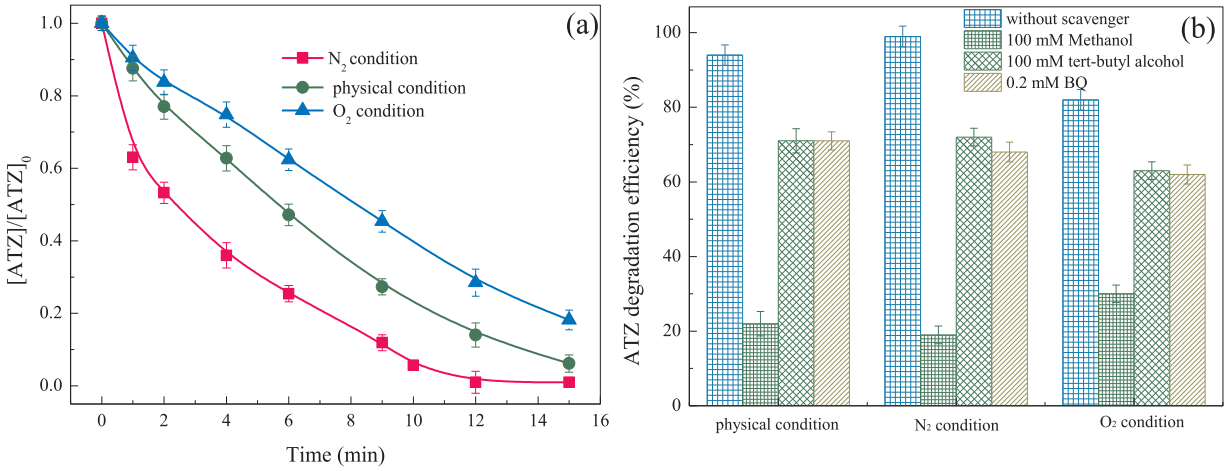

Fig. 4. (a) Atrazine degradation in Fe_3O_4/PMS/HA system under different aeration conditions, (b) the effects of radical scavengers on atrazine degradation in the Fe_3O_4/PMS/HA systems under different aeration conditions. Experiment conditions: $[atrazine]_0$ = 23 μM, $[Fe_3O_4]_0$ = 0.69 g/L, $[HA]_0$ = 0.3 mM, $[PMS]_0$ = 0.4 mM, initial pH = 6.8 (without buffer), and reaction time = 15 min.

peroxide could activate hydroxylamine to produce hydroxyl radical used for pollutant degradation. Herein, the concentration of hydrogen peroxide was determined to check whether Fe_3O_4/PMS Fenton-like occurred and had an effect on atrazine degradation. Surprisingly, it is found no hydrogen peroxide was detected in the Fe_3O_4/PMS/HA, and Fe_3O_4/PMS/HA-O_2 systems (Fig. S11), and the degradation of atrazine in the presence of molecular oxygen by Fenton-like reaction was excluded. In addition, in this study, the possibility that hydrogen peroxide decomposes hydroxylamine to reduce the residual amount of hydroxylamine in the solution and thus reduces the cycle of Fe(III)/Fe(II) is also ruled out. Furthermore, to fully explore the reason for atrazine degradation under different aeration conditions, the total iron ions were detected, and about 0.04 mg/L total iron ions were determined in the Fe_3O_4/PMS/HA system with N_2 condition, physical condition, and O_2 condition. Meanwhile, there was no detectable amount of dissolved Fe^{3+} was determined. That is to say, the 0.04 mg/L total iron ion was present in the form of Fe^{2+} in the presence of HA. Thus, we setup the Fe^{2+}/PMS/HA system to study the contribution of the dissolved Fe^{2+} to the atrazine degradation, and about 50% atrazine was degraded during the 15 min treatment (Fig. S12), which is only a little higher than the atrazine degradation by HA/PMS system (40%). The result shows that the trace amount of Fe^{2+} was not the major reason for the atrazine degradation.

$$O_2+2H^++2e^-\rightarrow H_2O_2 \quad (4)$$

$$2NH_2OH+O_2\rightarrow N_2+2H_2O+H_2O_2 \quad (5)$$

As identified above, it is thus inferred that the reduced molecular oxygen in the reaction solution accelerated the successive recycle of surface Fe(III)/Fe(II) on Fe_3O_4. To further verify this speculation, we investigated the Fe_3O_4 reduction process by monitoring the chemical state changes of iron species on Fe_3O_4 surface in Fe_3O_4/PMS/HA system under different aeration conditions. X-ray photoelectron spectroscopy (XPS) was used to analyze the surface information of Fe_3O_4 before and after atrazine degradation in Fe_3O_4/PMS/HA system under the physical condition, N_2 condition, and O_2 condition, the results are shown in Fig. 5. The survey XPS spectra displayed carbon (C 1s), iron (2p), and oxygen (1s) elements on the surface of Fe_3O_4 with the C 1s binding energy at 284.8 eV (Fig. 5(a), (d), (g), and (j)). In this study, for Fe_3O_4 catalyst used in all the three reaction systems under different aeration conditions, the binding energies of Fe $2p_{3/2}$ and Fe $2p_{1/2}$ are consistent with that reported in the literatures, locating at 711.0 and 724.6 eV, respectively [47–49]. The Fe $2p_{3/2}$ peak of the Fe_3O_4 was fitted with two peaks with peaks position at 710.5 and 712.1 eV, which were ascribed to the Fe(II) and Fe(III) on the surface sites [50]. Meanwhile, the molar ratio of ferrous iron to the total (Fe(II)/Fe_{total}) and the ferric iron to the total iron (Fe(III)/Fe_{total}) was calculated according to the fitting peak areas of Fe 2p core level spectra, respectively (Table S2). It is noted that the fresh Fe_3O_4 process the Fe(II)/Fe_{total} 0.3328, which was very close to the theoretical value. Interesting, the molar ratio of the Fe (II)/Fe_{total} on the surface of used Fe_3O_4 in the Fe_3O_4/PMS/HA-N_2 system was significantly enhanced to 0.5356, increasing by 61%. For comparison, the values of Fe(II)/Fe_{total} of the used Fe_3O_4 in the Fe_3O_4/PMS/HA (0.4838), and Fe_3O_4/PMS/HA-O_2 (0.4586) systems were much lower than that of Fe_3O_4/PMS/HA-N_2 (0.5356) system, but still higher than that of the fresh Fe_3O_4 (0.3328). The result proved the added hydroxylamine in Fe_3O_4/PMS/HA system truly could accelerate the recovery of surface Fe (II) of catalyst, which could subsequently promote the PMS decomposition to generate more radicals for the atrazine degradation, but this promotion works best under anaerobic condition and decreases with the increase of molecules oxygen existed in the system. Nevertheless, the addition of hydroxylamine in the reaction system significantly improves the degradation of atrazine, whether under aerobic or anaerobic conditions.

Herein, in order to explore the role of oxygen species in the reaction process, the changes of XPS spectra of O 1s in the fresh and used Fe_3O_4 are compared (Fig. 5(c), (f), (i), and (l)). For all the three systems, the O 1s peak at 530.1 eV was assigned to the lattice oxygen (O_2^-) in the metal oxide [20,50]. Another peak at the binding energy of 531.6 eV belonged to the hydroxide (OH^-) in the surface hydroxyls [35,50]. And the peak at 533.2 eV was attributed to the adsorbed H_2O on the surface of Fe_3O_4 [35]. Based on the fitted peak areas of O 1s, the O_2^-, OH^-, and H_2O account 50.8%, 36.1% and 13.1% in the fresh Fe_3O_4 (Table S3), respectively. In sharp contrast, as the molecular oxygen concentration in the reaction system increases, the OH^- percentage increases, accompanied by the decreasing of the adsorbed H_2O. To be specific, compared with the fresh Fe_3O_4, the content of OH^- in Fe_3O_4/PMS/HA-N_2, Fe_3O_4/PMS/HA, and Fe_3O_4/PMS/HA-O_2 systems increased from 36.1% to 38.2%, 43.0%, and 54.4%, respectively, and the corresponding proportion of H_2O decreased from 13.1% to 12.5%, 9.2%, and 4.4%. The changes of the content of different species of oxygen indicated that the adsorbed H_2O and OH- on the surface of Fe_3O_4 catalyst involved the reaction process.

3.7. Transformation products of hydroxylamine in the Fe_3O_4/PMS/HA system under different aeration conditions

Since the molecular oxygen would affect the conversion process of hydroxylamine [51], the final transformation products (e.g., NO_2^-, NO_3^-, N_2O, and N_2) of the hydroxylamine in the Fe_3O_4/PMS/HA system under different aeration conditions were ascertained (Fig. 6). According to the conservation of mass, the total nitrogen (TN) content is constant and equal to the initial concentration of N-NH_2OH, that is 4.2 mg/L (0.3 mM) in this study. As can be noticed in Fig. 6, NH_2OH was converted quickly in the three aeration conditions and the N-NH_2OH consumption percentage in the Fe_3O_4/PMS/HA-N_2, Fe_3O_4/PMS/HA, and Fe_3O_4/PMS/HA-O_2 systems were 91%, 88%, and 70%, respectively, suggesting that the presence of molecular oxygen could slightly inhibit the decomposition of NH_2OH. Herein, the residual HA could be removed based on the recycle of Fe(II)/Fe(III) during prolonged reaction time or the addition of suitable concentration of PMS [13]. Meanwhile, Fig. 6 shows the generation of NO_2^- and NO_3^- in the Fe_3O_4/PMS/HA-N_2, Fe_3O_4/PMS/HA, and Fe_3O_4/PMS/HA-O_2 systems. There was no significant concentration difference in the formation of N-NO_2^- and N-NO_3^- in the three systems.

Importantly, it should be noted that, in the three reaction systems, the difference of the oxidation products of hydroxylamine in three systems mainly reflects on the change of produced concentration of N-N_2O and N-N_2. Specifically, the produced environmentally friendly gas of N-N_2 in the Fe_3O_4/PMS/HA-N_2 and Fe_3O_4/PMS/HA-O_2 systems were 3.4 mg/L and 2.4 mg/L, respectively, and the corresponding content percentage of N_2O in the above two systems are both 0.1 mg/L. In other words, in the Fe_3O_4/PMS/HA-N_2 and Fe_3O_4/PMS/HA-O_2 systems, 81% and 67% of the consumed N-NH_2OH are converted into the N_2, while the generated N-N_2O only account for 1.5%, respectively. For the contrast, regard to the reaction exposed to the physical condition (i.e., Fe_3O_4/PMS/HA system), the generated N-N_2 (1.4 mg/L) significantly reduced by 59% and 42% compared with Fe_3O_4/PMS/HA-N_2 and Fe_3O_4/PMS/HA-O_2 systems, as well as N-N_2O (1.9 mg/L) significantly increased by 18 times. The above results indicated that oxygen-rich and anaerobic conditions are more conducive to the conversion of hydroxylamine to N-N_2 products, while hydroxylamine is more readily converted to N-N_2O under atmospheric condition, which was in accordance with the oxidation of hydroxylamine in the aqueous by the hydroxyl radical [51]. The results of oxidation products of hydroxylamine suggested that single-electron oxidations of hydroxylamine into N_2 was the dominant way in the Fe_3O_4/PMS/HA system under O_2 and N_2 conditions (Eq. (6)), while two-electron oxidations of hydroxylamine into N_2O play an important role under the physical condition (Eq. (7)) [15,16,52,53]. In addition, the generation of N_2 in the absence of O_2 was favored through Eq. (8) [51]. Subsequently, the NO_2^- and NO_3^- were produced when reactions (9)-(11) happened in the reaction

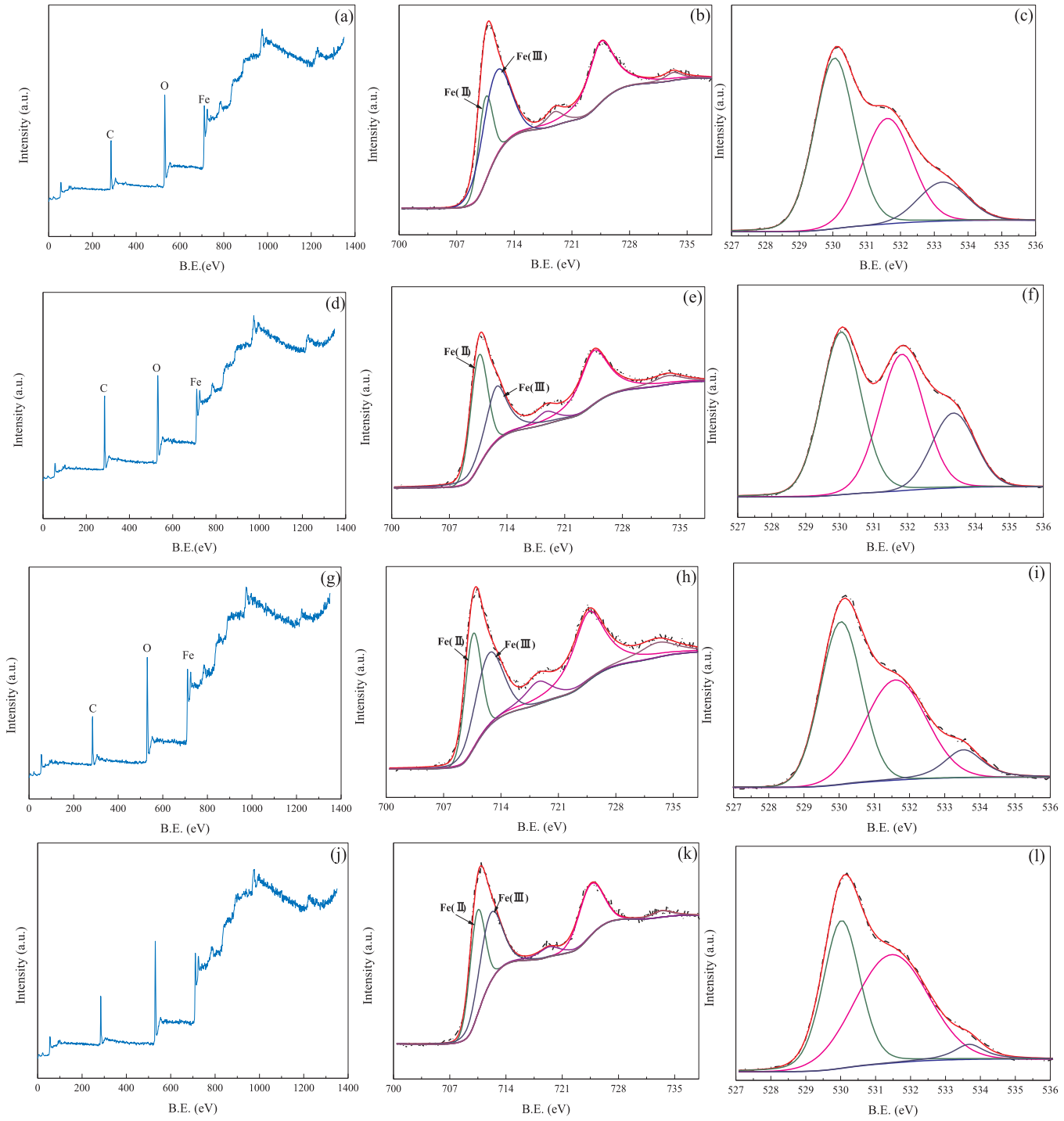

Fig. 5. XPS spectra of fresh (a–c) and reacted Fe_3O_4 (d–l) in Fe_3O_4/PMS/HA system under different atmospheric conditions: (d–f) N_2 condition, (g–i) physical condition and (j–l) O_2 condition, respectively. (a, d, g, and j) full-range scan of the samples, (b, e, h, and k) Fe 2p core level, and (c, f, i, and l) O 1s core level.

solution of Fe_3O_4/PMS/HA system under different aeration conditions [13].

$$Fe(III)+NH_3OH^+ \rightarrow Fe(II)+1/2N_2+2H^++H_2O \quad (6)$$

$$2Fe(III)+NH_3OH^+ \rightarrow 2Fe(II)+1/2N_2O+3H^++1/2H_2O \quad (7)$$

$$NHO+NH_2OH \rightarrow N_2+2H_2O \quad (8)$$

$$Fe(III)+NH_2OH \rightarrow NH_2O^{\bullet}+Fe(II)+H^+ \quad (9)$$

$$5Fe(III)+2H_2O+NH_2O^{\bullet} \rightarrow NO_3^-+5Fe(II)+6H^+ \quad (10)$$

$$NO_3^-+NH_2OH+OH^- \rightarrow NO^-+NO_2^-+H_2O \quad (11)$$

3.8. Effect of common inorganic anions on atrazine degradation

The existing anions including Cl^-, NO_3^-, HCO_3^-, and HPO_4^{2-}, are commonly present in the aquatic environment. Firstly, the effect of different chloride ion (Cl^-) concentration on atrazine degradation was explored in Fe_3O_4/PMS/HA system. It was observed that atrazine degradation efficiency reduced from 94% to 82% in the presence of 10 mM Cl^- (Fig. S13(a)). The chlorine radical ($Cl_2^{\bullet-}$) could be

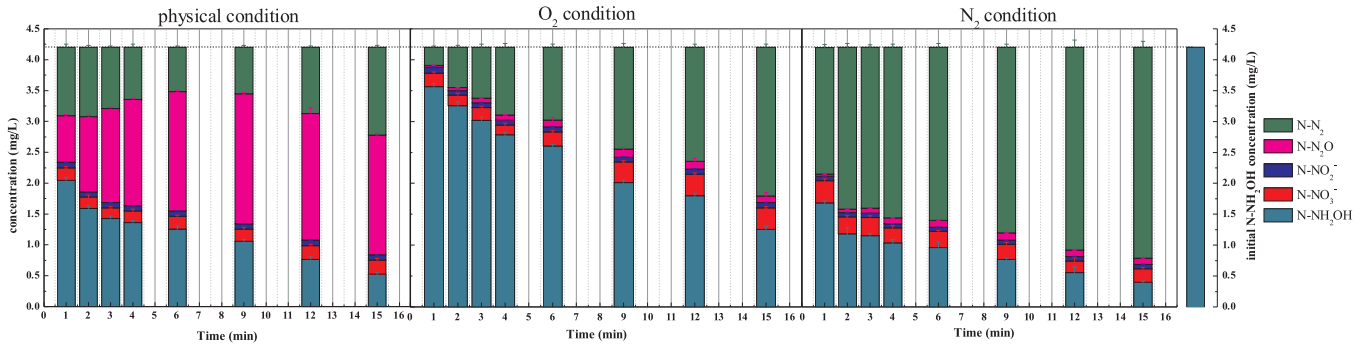

Fig. 6. The final transformation products of HA in Fe_3O_4/PMS/HA system. Experiment conditions: $[atrazine]_0$ = 23 μM, $[Fe_3O_4]_0$ = 0.69 g/L, $[HA]_0$ = 0.3 mM, $[PMS]_0$ = 0.4 mM, initial pH = 6.8 (without buffer), and reaction time = 15 min.

generated by the interaction between sulfate radical/hydroxyl radical and chloride with the reaction rate constant of 2.47×10^8 $M^{-1}s^{-1}$/ $(6.1 \pm 0.8) \times 10^9$ $M^{-1}s^{-1}$ (Eqs. (12) and (13)) [54]. Because the redox potential of produced chlorine radical ($E^0(Cl_2^{\bullet-}/2Cl^-)$ = 2.09 V) is lower than sulfate radical ($E^0(SO_4^{\bullet-}/SO_4^{2-})$ = 2.5–3.1 V), the presence of chloride in solution reduced the oxidation capacity of sulfate radical/ hydroxyl radical. Similarly, as observed in Fig. S13(b), a slight decrease in the atrazine degradation efficiency (from 94% to 85%) was exhibited when the concentration of nitrate (NO_3^-) in Fe_3O_4/PMS/HA process increased from 0 mM to 10 mM, which is attributed to the scavenging reactions between NO_3^- and $SO_4^{\bullet-}$/$HO^\bullet$ (Eqs. (14) and (15)) produced the nitrate radicals ($NO_3^\bullet$) with low reactivity [54].

$$SO_4^{\bullet-} + Cl^- \rightarrow Cl^\bullet + SO_4^{2-},\ k = 2.47 \times 10^8\ M^{-1}S^{-1} \quad (12)$$

$$HO^{\bullet-} + Cl^- \rightarrow HOCl^{\bullet-},\ k_f = (6.1 \pm 0.8) \times 10^9\ M^{-1}\ S^{-1} \quad (13)$$

$$HO^\bullet + NO_3^- \rightarrow OH^- + NO_3^\bullet,\ k < 5.5 \times 10^5 M^{-1}s^{-1} \quad (14)$$

$$SO_4^{\bullet-} + NO_3^- \rightarrow NO_3^\bullet + SO_4^{2-},\ k = 5.5 \times 10^5 M^{-1}\ S^{-1} \quad (15)$$

Bicarbonate ion (HCO_3^-) and hydrogen phosphate ion (HPO_4^{2-}) are also the representative inorganic ions existed in natural water. Herein, we also investigated the effects of HCO_3^-/HPO_4^{2-} on the atrazine degradation in the Fe_3O_4/PMS/HA system. Meanwhile, in order to avoid the rise of the solution pH caused by the addition of HCO_3^-/ HPO_4^{2-}, 1 mM acetate buffer was adopted to control the solution pH at 4.0. In the Fe_3O_4/PMS/HA system, as the HCO_3^- appeared in the reaction solution and increased from 0 to 1.0 mM, the atrazine degradation efficiency reduced from 95% to 53% (Fig. S13 (c)) due to the radical quenching reactions between hydroxyl radicals/sulfate radicals and HCO_3^- (Eqs. (16) and (17)) [55]. In addition, the HCO_3^- could as the metal complexing agent to affect the surface properties of metals, thereby inhibiting the degradation process [56]. What's more, in Fig, S13(d), the atrazine degradation efficiency dramatically decreased to 14% in the presence of 1.0 mM HPO_4^{2-}, which mainly ascribed to the following points: one is that HPO_4^{2-} would coordinate with transition metals on the surface of the catalyst, making an inhibition effect on the pollutant degradation process [57,58]. What's more, HPO_4^{2-} reacts with hydroxyl radicals/sulfate radicals to form weaker radicals (e.g., $PO_4^{\bullet2-}$ and $HPO_4^{\bullet-}$) (Eqs. (18) and (19)) [55]. As we all known, the natural organic matter (NOM) in the wastewater would consume active radicals in the AOPs. Herein, we also studied the effect of different concentration of humic acid (a typical NOM) on atrazine degradation. As shown in the Fig. S13 (e), the atrazine degradation efficiency decreased with humic acid concentration increasing from 0 to 10 mg/L, the reason mainly ascribed that humic acid would react with $HO^\bullet$ and $SO_4^{\bullet-}$ ((Eqs. (20) and (21)), reducing the amount of active radicals [59,60].

$$HO^\bullet + HCO_3^- \rightarrow OH^- + HCO_3^{\bullet-},\ k = 8.5 \times 10^8\ M^{-1}s^{-1} \quad (16)$$

$$SO_4^{\bullet-} + HCO_3^- \rightarrow HCO_3^{\bullet-} + SO_4^{2-},\ k = 9.1 \times 10^6\ M^{-1}s^{-1} \quad (17)$$

$$SO_4^{\bullet-} + HPO_4^{2-} \rightarrow PO_4^{\bullet2-} + SO_4^{2-} + H^+,\ k = (1.2 \pm 0.3) \times 10^{16} M^{-1}s^{-1} \quad (18)$$

$$HO^\bullet + HPO_4^{2-} \rightarrow HPO_4^{\bullet-} + OH^-,\ k = (1.5 \pm 0.3) \times 10^6\ M^{-1}s^{-1} \quad (19)$$

$$SO_4^{\bullet-} + NOM \rightarrow \text{products},\ k = 2.35 \times 10^7\ M^{-1}s^{-1} \quad (20)$$

$$HO^\bullet + NOM \rightarrow \text{products},\ k = 3 \times 10^8\ M^{-1}s^{-1} \quad (21)$$

3.9. Possible activation reaction mechanism of the Fe_3O_4/PMS/HA process

Based on the above analysis, two major reaction mechanisms of Fe_3O_4/PMS/HA process for atrazine degradation are proposed (Fig. 7):

(i) The accelerated recycle of surface Fe(III)/Fe(II) through hydroxylamine reduction: when metallic oxide was mixed with water, the surface of oxide easily adsorbs H_2O molecules. Since water molecules are readily dissociated into OH^- and H^+, hydroxyl groups prevalently existed on the surface sites as ligands [58], which was in accordance with our XPS results (Fig. 5). For the PMS activation by Fe_3O_4 catalyst, the H_2O molecule was first physically adsorbed on the active sites of Fe(II) located on the surface of the Fe_3O_4 catalyst and formed the $\equiv Fe(II) - OH^-$. In the process of interacting with PMS, the surface $\equiv Fe(II) - OH^-$ firstly reacted with PMS to generate $SO_4^{\bullet-}$ and $HO^\bullet$ (Eqs. (22)–(24)). Meanwhile, a small number of hydroxyl radicals were also generated in our reaction process through the reaction between sulfate radical and H_2O (Eq. (25)) [29]. In addition, it was believed that the effectiveness of the catalytic PMS oxidation by metal ions (M^{n+}) depended on the regeneration of M^{n+} from M^{n+1} [39]. In our study, Fe (II) would transform to Fe(III) through oxidation process. Similarly, some literatures have reported that the reactivity of $\equiv Fe(III)$ for PMS activation is weak, and the reduction from $\equiv Fe(III)$ to $\equiv Fe(II)$ was regarded to be the rate-determining step [13,61]. Herein, in our study, the regeneration of $\equiv Fe(II)$ was obviously accelerated by the added

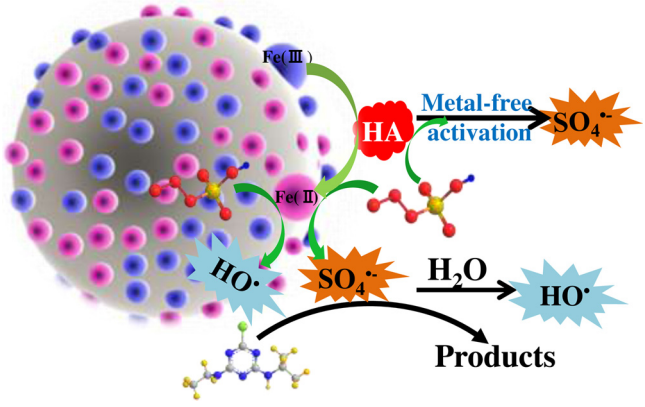

Fig. 7. The reaction mechanism of Fe_3O_4/PMS/HA system.

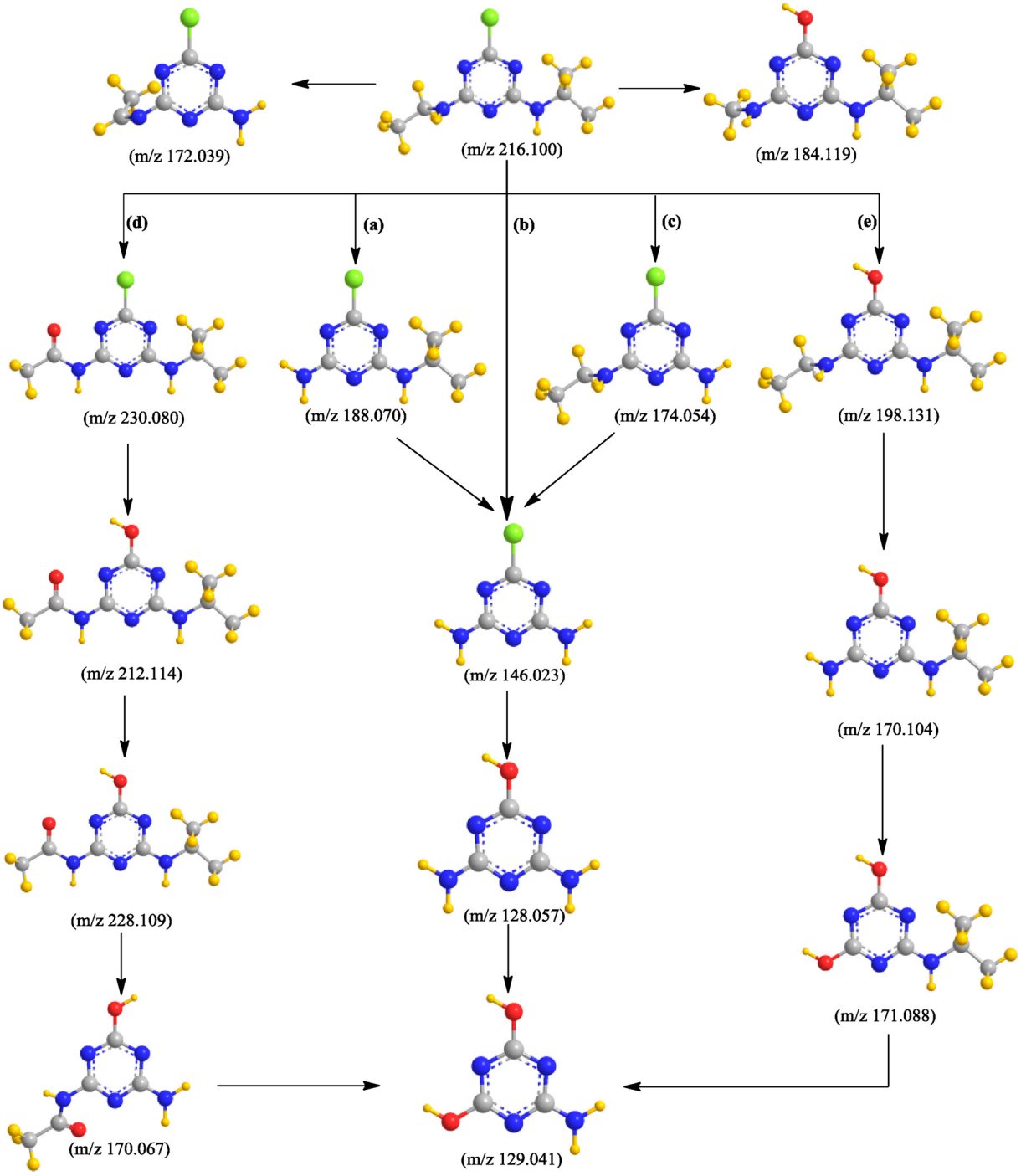

Fig. 8. The atrazine degradation pathways in Fe_3O_4/PMS/HA system.

hydroxylamine. That is, the surface ≡Fe(III) could be subsequently reduced to surface ≡Fe(II) by hydroxylamine (Eq. (26)) [13,18,62]. Subsequently, the nascent ≡Fe(II) recycles the reactions (22)–(25) to continually generate free radicals.

(ii) The direct activation of PMS in homogeneous catalytic oxidation: The metal-free activation of PMS by hydroxylamine (Eq. (27)) to generate free radicals for atrazine degradation occurred in our study (Fig. 2(b)), which was in accordance with the study of Feng et al. [23]. In addition, the trace Fe^{2+} has a slight contribution to the atrazine degradation, which is only 10% higher than that in HA/PMS system.

$$\equiv Fe(II)\text{-}OH^- + HSO_5^- \rightarrow \equiv Fe(III) + HO^{\bullet} + SO_4^{2-} \quad (22)$$

$$\equiv Fe(II)\text{-}OH^- + HSO_5^- \rightarrow \equiv Fe(III) - (HO)OSO_3^- + OH^- \quad (23)$$

$$\equiv Fe(II) - (HO)OSO_3^- \rightarrow \equiv Fe(III)\text{-}OH^- + SO_4^{\bullet -} \quad (24)$$

$$SO_4^{\bullet -} + H_2O \rightarrow HO^{\bullet} + H^+ + SO_4^{2-} \quad (25)$$

$$\equiv Fe(III)\text{-}OH + NH_2OH \rightarrow \equiv Fe(II)\text{-}OH + NH_2O^{\bullet} + H^+ \quad (26)$$

$$HSO_5^- + NH_2OH \rightarrow SO_4^{\bullet -} + NH_2O^{\bullet} + H_2O \quad (27)$$

3.10. Degradation intermediates and degradation pathways of atrazine

In this study, the degradation products of atrazine **(1)** were determined by LC-QTOF-MS/MS, and 13 degradation intermediates were

measured finally (Table S4), including 4-amino-6-(isopropylamino)-1,3,5-triazin-2-ol (m/z +170.104, OAIT) **(2)**, 4,6-diamino-1,3,5-triazin-2-ol (m/z +128.057, OAAT) **(3)**, 6-chloro-N^2-ethyl-1,3,5-triazine-2,4-diamine (m/z +174.054, DIA) **(4)**, 2-chloro-4,6-diamino-1,3,5-triazine (m/z +146.023, CAAT) **(5)**, 2-chloro-4-amino-6-isopropylamino-1,3,5-triazine (m/z +188.070, CAIT) **(6)**, N-(4-chloro-6-(isopropylamino)-1,3,5-triazin-2-yl) acetamide (m/z +230.080, CDIT) **(7)**, N-(4-hydroxy-6-(isopropylamino)-1,3,5-triazin-2-yl) acetamide (m/z +212.114, ODIT) **(8)**, 4-(isopropylamino)-6-(methylamino)-1,3,5-triazin-2-ol (m/z +184.119, OMIT) **(9)**, 6-(isopropylamino)-1,3,5-triazine-2,4-diol (m/z +171.008, OOIT) **(10)**, (E)-6-chloro-N2-ethylidene-1,3,5-triazine-2,4-diamine (m/z +172.039, CVIT) **(11)**, 6-amino-1,3,5-triazine-2,4-diol (m/z +129.041, OOAT) **(12)**, N-(4-hydroxy-6-((2-hydroxypropan-2-yl)amino)-1,3,5-triazin-2-yl)acetamide (m/z +228.109, ODHT) **(13)**, and N-(4-amino-6-hydroxy-1,3,5-triazin-2-yl)acetamide (m/z +170.067, ODAT) **(14)**. The TIC and the MS/MS products of the detected intermediates were exhibited in Figs. S14–28.

The above detected degradation products indicated that the atrazine degradation involving the dealkylation, dechlorination-hydroxylation, alkylic-oxidation, alkylic-hydroxylation, deamination-hydroxylation, and olefination, as exhibited in Fig. 8. Firstly, sulfate radical as the electrophilic oxidant could attack the electron-rich part of the atrazine through electron transfer to generate dealkylation degradation products including CAIT (m/z + 188.070), DIA (m/z + 174.054), and CAAT (m/z + 146.023) [63]. The H-abstraction caused by free radicals ($HO^{\bullet}$ and $SO_4^{\bullet-}$) from lateral chains of atrazine can lead to the generation of CVAT (m/z + 172.039) olefination products. Meanwhile, hydroxyl radicals could lead to an alkylic-oxidation process by attacking the N-adjacent carbon atom of the alkylic lateral chain, which could form the CDIT (m/z + 230.080) by-product [64]. In addition, it has been reported that the bond length of C–Cl bond in atrazine (1.734 Å) was the longest among the whole molecular structure, however, the polarity linked with this bond is low [65]. Thus, the cleavage of this bond is the easiest and another possible degradation pathway was the formation of OEIT (m/z + 198.131), ODIT (m/z + 212.114) and OAAT (m/z + 128.057) through dechlorination-hydroxylation by the substitution of the chlorine atom by hydroxyl group. Subsequently, the continuous oxidation by hydroxyl radical resulted in the generation of alkylic-hydroxylation byproducts of ODHT (m/z + 228.109). Subsequently, the OAIT (m/z + 170.104) was formed from the de-ethylation process, then, OAIT (m/z + 170.104) and OAAT (m/z + 128.057) undergo deamination-hydroxylation to form OOIT and (m/z + 171.088) and OOAT (m/z + 129.041), respectively. Further oxidation also transfer ODAT (m/z + 170.067) into the final degradation intermediate OOAT (m/z + 129.041).

4. Conclusions

We have found that the efficient atrazine degradation was achieved in the Fe_3O_4/PMS Fenton-like heterogeneous system in the presence of hydroxylamine under near-neutral pH (5.0–6.8, without buffer). The enhanced atrazine degradation in the Fe_3O_4/PMS/HA system was mainly attributed to the accelerated Fe(III)/Fe(II) recycle on Fe_3O_4 surface caused by hydroxylamine, which was verified by the X-ray photoelectron spectroscopy (XPS) analysis of the fresh and used Fe_3O_4. Compared to oxygen-rich and physical conditions, anaerobic condition was more beneficial to the regeneration of surface Fe(II) on the surface of Fe_3O_4, obviously promoting the atrazine degradation rate. In addition, the role of hydroxylamine as a reducing agent or activator in Fe_3O_4/PMS/HA system would change with the content of hydroxylamine. In this study, the metal-free PMS activation with HA also contributed to the destruction of atrazine (40%). What's more, in the Fe_3O_4/PMS/HA system, hydroxylamine was more susceptible to single-electron reactions under O_2 and N_2 conditions, and two-electron reactions occurred under the physical condition. Sulfate radical and hydroxyl radical mainly contribute to the atrazine degradation. The results of this study provided a method for promoting the efficiency of the iron oxide-based heterogeneous process used for the degradation of organic pollutants in the environment.

Acknowledgment

The authors would like to acknowledge the financial support from National Natural Science Foundation of China (No. 51878423) and Graduate Student's Research and Innovation Fund of Sichuan University (No. 2018YJSY075).

Appendix A. Supplementary data

Supplementary material related to this article can be found, in the online version, at doi:https://doi.org/10.1016/j.apcatb.2019.117782.

References

[1] B. Balci, N. Oturan, R. Cherrier, M.A. Oturan, Water Res. 43 (2009) 1924–1934.
[2] X. Kong, J. Jiang, J. Ma, Y. Yang, W. Liu, Y. Liu, Water Res. 90 (2016) 15–23.
[3] J. Peng, X. Lu, X. Jiang, Y. Zhang, Q. Chen, B. Lai, G. Yao, Chem. Eng. J. 354 (2018) 740–752.
[4] D. Wang, H. Xu, J. Ma, X. Lu, J. Qi, S. Song, Chem. Eng. J. 354 (2018) 113–125.
[5] Z. Yang, A. Yu, C. Shan, G. Gao, B. Pan, Water Res. 137 (2018) 37–46.
[6] J. Wang, S. Wang, Chem. Eng. J. 334 (2018) 1502–1517.
[7] P. Hu, M. Long, Appl. Catal. B 181 (2016) 103–117.
[8] F. Ji, H. Zhang, X. Wei, Y. Zhang, B. Lai, Chem. Eng. J. 359 (2019) 1316–1326.
[9] Z. Xiong, H. Zhang, W. Zhang, B. Lai, G. Yao, Chem. Eng. J. 359 (2019) 13–31.
[10] H.D. Xu, D. Wang, J. Ma, T. Zhang, X.H. Lu, Z.Q. Chen, Appl Catal B-environ 238 (2018) 557–567.
[11] C. Li, Y. Huang, X. Dong, Z. Sun, X. Duan, B. Ren, S. Zheng, D.D. Dionysiou, Appl. Catal. B 247 (2019) 10–23.
[12] A. Rastogi, S.R. Al-Abed, D.D. Dionysiou, Appl. Catal. B 85 (2009) 171–179.
[13] J. Zou, J. Ma, L. Chen, X. Li, Y. Guan, P. Xie, C. Pan, Environ. Sci. Technol. 47 (2013) 11685–11691.
[14] G. Liu, X. Li, B. Han, L. Chen, L. Zhu, L.C. Campos, J. Hazard. Mater. 322 (2017) 461–468.
[15] L. Chen, J. Ma, X. Li, J. Zhang, J. Fang, Y. Guan, P. Xie, Environ. Sci. Technol. 45 (2011) 3925–3930.
[16] H. Lee, H.J. Lee, J. Seo, H.E. Kim, Y.K. Shin, J.H. Kim, C. Lee, Environ. Sci. Technol. 50 (2016) 8231–8238.
[17] J. Yan, J. Peng, L. Lai, F. Ji, Y. Zhang, B. Lai, Q. Chen, G. Yao, X. Chen, L. Song, Environ. Sci. Technol. (2018).
[18] X. Hou, X. Huang, F. Jia, Z. Ai, J. Zhao, L. Zhang, Environ. Sci. Technol. 51 (2017) 5118–5126.
[19] W. Liu, Y. Wang, Z. Ai, L. Zhang, ACS Appl. Mater. Interfaces 7 (2015) 28534–28544.
[20] X. Hu, B. Liu, Y. Deng, H. Chen, S. Luo, C. Sun, P. Yang, S. Yang, Appl. Catal. B 107 (2011) 274–283.
[21] J. Zhang, M. Chen, L. Zhu, RSC Adv. 6 (2016) 47562–47569.
[22] D. Sannino, V. Vaiano, P. Ciambelli, L.A. Isupova, Chem. Eng. J. 224 (2013) 53–58.
[23] Y. Feng, D. Wu, Y. Zhou, K. Shih, Chem. Eng. J. 330 (2017) 906–913.
[24] Y. Leng, W. Guo, X. Shi, Y. Li, A. Wang, F. Hao, L. Xing, Chem. Eng. J. 240 (2014) 338–343.
[25] W.-D. Oh, Z. Dong, T.-T. Lim, Appl. Catal. B 194 (2016) 169–201.
[26] Y.-H. Guan, J. Ma, Y.-M. Ren, Y.-L. Liu, J.-Y. Xiao, L.-q. Lin, C. Zhang, Water Res. 47 (2013) 5431–5438.
[27] J. Yan, J. Li, J. Peng, H. Zhang, Y. Zhang, B. Lai, Chem. Eng. J. 359 (2019) 1097–1110.
[28] P. Neta, R. Huie, A.B. Ross, Rate Constants for Reactions of Inorganic Radicals in Aqueous-Solution (1988).
[29] Y. Ding, L. Zhu, N. Wang, H. Tang, Appl. Catal. B 129 (2013) 153–162.
[30] W.D. Oh, Z. Dong, G. Ronn, T.T. Lim, J. Hazard. Mater. 325 (2017) 71–81.
[31] Z. Chen, J. Jin, X. Song, G. Zhang, S. Zhang, Environ. Sci. Technol. 52 (2018) 10011–10018.
[32] X. Cheng, H. Guo, Y. Zhang, X. Wu, Y. Liu, Water Res. 113 (2017) 80–88.
[33] Y. Qian, X. Zhou, Y. Zhang, W. Zhang, J. Chen, Chemosphere 91 (2013) 717–723.
[34] D. Xia, Y. Li, G. Huang, R. Yin, T. An, G. Li, H. Zhao, A. Lu, P.K. Wong, Water Res. 112 (2017) 236–247.
[35] C. Tan, N. Gao, Y. Deng, J. Deng, S. Zhou, J. Li, X. Xin, J. Hazard. Mater. 276 (2014) 452–460.
[36] C. Luo, J. Ma, J. Jiang, Y. Liu, Y. Song, Y. Yang, Y. Guan, D. Wu, Water Res. 80 (2015) 99–108.
[37] M.N. Hughes, H.G. Nicklin, Journal of the Chemical Society A Inorganic Physical Theoretical (1971) 3485–3487.
[38] G.V. Buxton, C.L. Greenstock, W.P. Helman, A.B. Ross, J. Phys. Chem. Ref. Data 17 (1988) 513–886.
[39] T. Zhang, H. Zhu, J.-P. Croué, Environ. Sci. Technol. 47 (2013) 2784–2791.
[40] Y.H. Guan, J. Ma, X.C. Li, J.Y. Fang, L.W. Chen, Environ. Sci. Technol. 45 (2011) 9308–9314.

[41] T. Zhang, Y. Chen, Y. Wang, J. Le Roux, Y. Yang, J.-P. Croué, Environ. Sci. Technol. 48 (2014) 5868–5875.
[42] G. Ying-Hong, M. Jun, L. Xu-Chun, F. Jing-Yun, C. Li-Wei, Environ. Sci. Technol. 45 (2011) 9308.
[43] R.C. Thompson, Inorg. Chem. 20 (1981).
[44] H. Zhao, Y. Wang, Y. Wang, T. Cao, G. Zhao, Appl Catal B-environ 125 (2012) 120–127.
[45] G.-D. Fang, D.D. Dionysiou, S.R. Al-Abed, D.-M. Zhou, Appl. Catal. B 129 (2013) 325–332.
[46] L. Chen, X. Li, J. Zhang, J. Fang, Y. Huang, P. Wang, J. Ma, Environ. Sci. Technol. 49 (2015) 10373–10379.
[47] Y. Liu, Y. Wang, S. Zhou, S. Lou, L. Yuan, T. Gao, X. Wu, X. Shi, K. Wang, ACS Appl. Mater. Interfaces 4 (2012) 4913–4920.
[48] B.Y. Yu, S.-Y. Kwak, J. Mater. Chem. 20 (2010) 8320–8328.
[49] P. Yuan, D. Liu, M. Fan, D. Yang, R. Zhu, F. Ge, J. Zhu, H. He, J. Hazard. Mater. 173 (2010) 614–621.
[50] L. Xu, J. Wang, Environ. Sci. Technol. 46 (2012) 10145–10153.
[51] N.K.V. Leitner, P. Berger, G. Dutois, B. Legube, J. Photochem. Photobiol. A: Chem. 129 (1999) 105–110.
[52] G. Bengtsson, S. Fronæus, L. Bengtsson-Kloo, J. Chem. Soc. Dalton Trans. (2002) 2548–2552.
[53] J.H. Butler, L.I. Gordon, Inorg. Chem. 25 (1986) 4573–4577.
[54] T. Zhou, X. Zou, J. Mao, X. Wu, Appl. Catal. B 185 (2016) 31–41.
[55] J.-C.E. Yang, B. Yuan, H.-J. Cui, S. Wang, M.-L. Fu, Appl Catal B-environ 205 (2017) 327–339.
[56] J.-C.E. Yang, B. Yuan, H.-J. Cui, S. Wang, M.-L. Fu, Appl. Catal. B 205 (2017) 327–339.
[57] G.-X. Huang, C.-Y. Wang, C.-W. Yang, P.-C. Guo, H.-Q. Yu, Environ. Sci. Technol. 51 (2017) 12611–12618.
[58] T. Zhang, C. Li, J. Ma, H. Tian, Z. Qiang, Appl. Catal. B 82 (2008) 131–137.
[59] P. Xie, J. Ma, W. Liu, J. Zou, S. Yue, X. Li, M.R. Wiesner, J. Fang, Water Res. 69 (2015) 223–233.
[60] L. Chen, D. Ding, C. Liu, H. Cai, Y. Qu, S. Yang, Y. Gao, T. Cai, Chem. Eng. J. 334 (2018) 273–284.
[61] Y. Feng, D. Wu, Y. Deng, T. Zhang, K. Shih, Environ. Sci. Technol. 50 (2016) 3119–3127.
[62] M.D. Johnson, B.J. Hornstein, Inorg. Chem. 42 (2003) 6923–6928.
[63] H. Zhang, X. Liu, J. Ma, C. Lin, C. Qi, X. Li, Z. Zhou, G. Fan, J. Hazard. Mater. 344 (2018) 1220–1228.
[64] Y. Huang, C. Han, Y. Liu, M.N. Nadagouda, L. Machala, K.E. O'Shea, V.K. Sharma, D.D. Dionysiou, Appl. Catal. B 221 (2018) 380–392.
[65] C. Chen, S. Yang, Y. Guo, C. Sun, C. Gu, B. Xu, J. Hazard. Mater. 172 (2009) 675–684.